Characterization of a UV-USP laser grooving process combined with plasma dicing to support next generation advanced packaging trends

Rogier Evertsen[1], Janet Hopkins[2], Oliver Ansell[2], Samira Kazemi[2], Roland Mumford[2], Richard Barnett[2], Kees Biesheuvel[1], Jeroen van Borkulo[1]
[1]ASMPT ALSI B.V., Platinawerf 20, 6641 TL Beuningen, The Netherlands
Email: rogier.evertsen@asmpt.com
[2]KLA Corporation (SPTS Division), Ringland Way, Newport, NP18 2TA, United Kingdom

Abstract
In this study, we investigated and characterized the combined process flow of the UV-USP (ultra-short pulse) laser grooving and plasma dicing wafer singulation technologies and discussed the impact on subsequent hybrid bonding steps. We benchmarked UV-USP laser grooving against UV-nanosecond laser grooving to enable plasma dicing by evaluation of imaging and die strength measurements. The results showed the advantages of the UV-USP laser grooving combined with plasma dicing for the current and future semiconductor production flows.

Key words
Hybrid bonding, die strength, plasma dicing, Si, UV-USP laser grooving.

I. Introduction
Wafer singulation using only blade dicing has been the workhorse in the industry for years but has shown many limitations [1] like chipping, cracking, a reduced die strength and such as a minimum street width and minimum die sizes. Consequently, several different die singulation technologies or combinations of technologies have been conceived for semiconductor production flows over the last couple of decades [1], [2].

Plasma dicing [3], [4] has shown to be a good option for thick and thin wafer singulation. The flow is based on the Bosch process, which has been the industrial standard for deep silicon etching [5]. It uses a series of alternating steps between polymer deposition for sidewall passivation, removal of the polymer from the etch front, and isotropic silicon etching. The technology does require a suitable mask and the absence of metals, polymers and oxides in the dicing street. The method of the mask definition has a huge impact on the quality of the plasma dicing process. Plasma dicing alone applied to photolithography defined dicing kerfs will return the cleanest die with the highest die strength. This is already running in mass production, specifically for simple front-end stacks such as in RFID products. However, significant investment in changing front-end process flows is required for products containing more complex front-end stacks with multiple redistribution layers (RDL) and planarization steps. It is probable that for some products it will never be economically viable to remove all metals from the dicing streets. Therefore, an additional enabling step is required to benefit from many of the advantages of plasma dicing and will enable the transition to plasma dicing for many more products. Protrusions, recast, and non-verticality of the grooved stack can create a deviation of the mask edge which impacts the plasma etch front.

The advantages of laser dicing in the nanosecond regime over blade dicing have been described elsewhere [6]. The laser method can be applied for full separation of the wafer or for the removal of part of the device build, such as in case of grooving or scribing. The advantages can then be further exploited by combining it with, for example, blade dicing improving singulated die quality and reducing cost.

In recent years, also ultra-short pulse (USP) laser processing has been available for production [7], [8]. The use of these lasers shows advantages of using ultra-short pulses compared to nanosecond pulses, which result in a different material removal mechanism and small to no heat affected zone (HAZ) in the material, low to no burr and a smooth groove bottom.

Among others, due to the steep cost increase for the device development and fabrication of advanced nodes, the development of 3D heterogenous integration combining these different nodes, has accelerated, but requires fast

interconnects and excellent thermal and power management. The advanced interconnect technology has progressed from wirebonding through flipchip and micro bumps to hybrid bonding such as Cu-Cu interconnect technologies [9]. From the majority of the singulation techniques, such as blade dicing, stealth dicing, laser dicing and plasma dicing, only the combination of the laser processing and plasma dicing may comply with the requirements essential to hybrid bonding processes. Laser dicing only may not fulfill the burr free edge quality, whereas plasma dicing needs a sharp mask and metal removal from the street. In this respect, it is expected that the mask quality created by UV-USP laser grooving, compared to the nanosecond laser grooving, will qualify for the plasma dicing singulation step. In this paper, we will benchmark UV-USP grooving against UV-nanosecond laser grooving in combination with plasma dicing. Additionally, we characterize the technologies and their impact on the subsequent hybrid bonding processing steps.

II. Description

A. Laser grooving system

The laser grooving was executed on LASER1205 systems from ASMPT. These systems are using the ASMPT's patented multibeam technology. Multibeam laser technology has been used for several years by many assembly and packaging companies [10]. This technology is easily adjustable to various applications by optimizing the laser beam patterns on the wafer, as depicted in Fig. 1. As the goal for all laser technologies is to balance the throughput versus the quality, optimizing the beam pattern enables improving the quality of the top surface and die side wall, reducing burr and HAZ, and increasing the die strength.

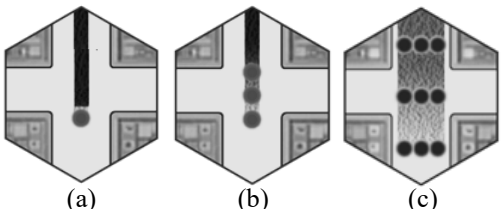

Figure 1: Examples of laser beam patterns in a dicing street. a) Single beam, b) multibeam in-line, c) advanced multibeam.

The laser removal process in the UV-ns laser regime is melt-driven. Material removal processes are fast, but the residual thermal energy introduces a relatively large melt pool and HAZ. UV-USP lasers operate with much shorter pulses with high pulse intensities. In this case, the material removal mechanism in these pico- to sub-pico regimes is not melt but ablation driven without requiring the material to go through a melt phase to enable removal. The HAZ is smaller and also the resolidified and deposited material is much lower, as depicted graphically in Fig. 2. For UV-USP laser processing, material absorption differences are less important, and metals, polymers, glasses and silicon removal rates are similar: with the same optical arrangement and spot sizes, UV-USP can achieve sharper, well defined grooves and edge sidewalls.

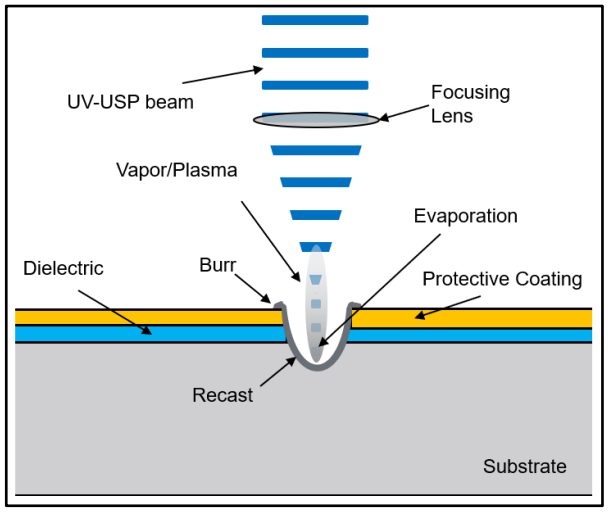

Figure 2: Schematic of UV-USP grooving

B. Plasma dicing system

The work described here was executed on an SPTS Rapier-300S process module attached to an SPTS 300 mm Mosaic^{TM} handler. This is a high density plasma source designed for high rate silicon etching. The samples were mounted on 400 mm outer diameter standard dicing frames using a dicing tape.

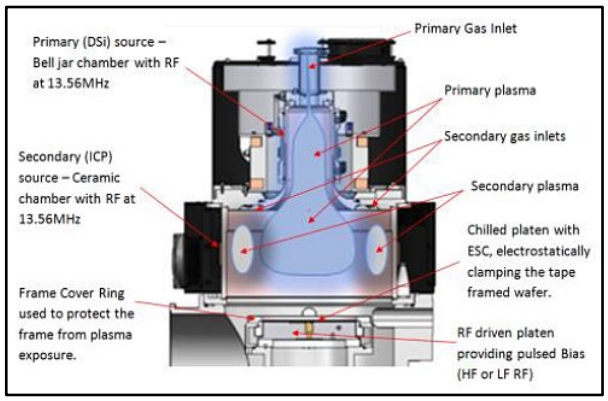

Figure 3: Schematic of plasma dicing module.

The process flow consisted of a pre-Bosch etch 'cleaning' or 'descum' step that removes small laser groove debris, the heat effected zone (HAZ). It creates a new, smooth boundary from where plasma dicing can start. A too long descum step undercuts the top layers which can break off and cause reliability issues. As the HAZ can contain micro cracks and voids, this can enhance the silicon etch rate in those areas to

create an undesired lateral etch as depicted in Fig. 4. An insufficient descum step (incomplete removal of HAZ) can cause striations and lateral etch. This should be avoided for optimum process control. Ideally the descum needs to be wide enough to remove the HAZ, but not so wide to promote delamination of the mask or stack layers.

The main plasma dicing process uses the Bosch process to etch down to the dicing tape. Endpoint detection hardware using optical emissions spectroscopy avoids excessive over-etch. A soft-landing process removes the remaining silicon slower to counter the loading effect as the Si reaches the tape, preventing damaging the sidewalls or the backside of the die and thereby maintaining the high die strength. The tuning of the etching is based on a compromise between scallop size, mask selectivity, productivity and lateral etch. Small scallops, as shown in Fig. 5b, tend to suppress lateral etching and may increase material strength [11].

The quality of the combined laser grooving and plasma dicing process requires the optimization of the laser process as well as the tuning of the plasma dicing process. For example, the definition of the mask and size of the HAZ will impact the descum step. Sample evaluation can be done on the burr, dimensions of the undercut and the occurrence of lateral etch. After the plasma dicing process, high pressure deionized water was used to remove the protective coating from the die surface. The dies were inspected using an Olympus MX50 optical microscope and a Zeiss Sigma FESEM.

C. *Material*

Experiments described here were performed on a test carrier of 150 µm double sided polished and etched Si substrate with 2 µm SiO_2. A water-soluble protective coat material is spun on the front side of the wafer (thickness of 4 to 5 µm) before the laser grooving processing takes place. For the experiments performed here, different groove widths and depths have been tested. The laser removed the top layer only and stop at the Si substrate, resulting in laser groove depths of about 3 µm. Sample size for die strength evaluation was 3 x 8 mm.

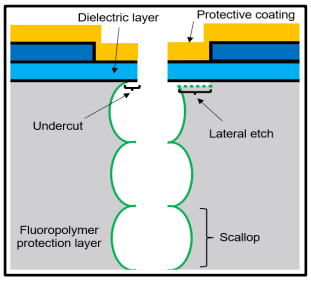

Figure 4: Schematic sideview of a sample after descum and several iterations of the Bosch process used in plasma dicing showing the typical scallops. Also shown are two quality indicators at the Si – dielectric interface: undercut and lateral etch.

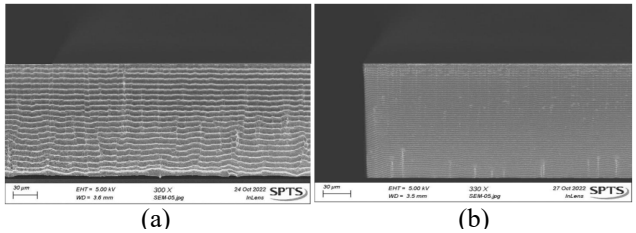

(a) (b)

Figure 5: Sidewall view of plasma diced Si sample with a) standard scallop size, and b) small scallop size.

D. *Analysis*

The material die strength was measured on a 3-point bending test tool [12], and both top and bottom distributions were evaluated. To obtain good position accuracy of the support and loading edges while preventing friction effects, a measurement jig with an air bearing was used. The die strength is calculated according to (1).

$$\text{Die strength (MPa)} = \frac{3FL}{2h^2d}. \quad (1)$$

where F is the breaking force in N, L is the distance between support bars in mm, h is the sample thickness in µm and d is the sample width in µm. For an acceptable indication of the distribution, N=15 samples per side were done.

III. Experiments

A. *Laser grooving of Si with SiO_2 top layer*

Laser grooving settings were optimized to minimize burr, edge delamination and depth for both laser systems. Fig. 6 shows the evaluation of the results of the UV-ns laser grooving after coating removal from the sample. The bottom of the groove has a regular, shiny appearance. The depth varies from 3.3 to 6.6 µm measured from the top surface with a maximum burr of 1.1 µm. The optically visible modification width of the surface groove edge is about 3.5 µm. The SEM inspection of a manually cleaved crosscut shows a groove profile with a wide w-shape. Zooming in at the edge, a small vertical trench deeper into the Si of about 2 µm is visible. The edge of the groove has no chippings, cracking or top layer delamination.

The result after UV-USP laser grooving after coating removal (Fig. 7) shows a very regular groove profile with a u-shape and a flat bottom. The depth varied from 3.9 to 4.1 µm measured from the top surface with a maximum burr of less than 300 nm. The optically visible modification width is about 4.0 µm. SEM images of a manually cleaved crosscut show the fine grainy nature of the groove bottom and the groove sidewall. Zooming in on the groove, no further modification of the silicon was visible, showing the control of the laser grooving depth. Also for UV-USP, the edge of the groove has no chipping, cracking or top layer delamination.

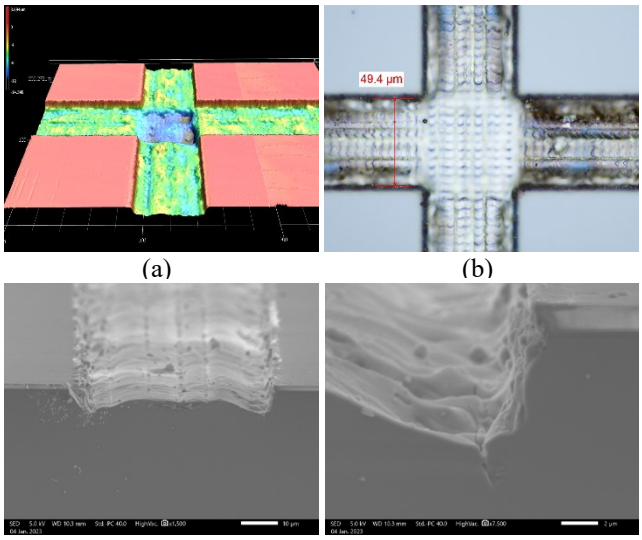

(a) (b) (c) (d)

Figure 6: Inspection of UV-ns laser grooved material after coating removal shows a smooth, shiny bottom and maximum burr of 1.1 µm with (a) confocal imaging and (b) optical microscopy. SEM inspection of a manually cleaved crosscut shows a groove profile (c) with a wide w-shape and zoomed in at the edge (d) a small vertical trench of about 2 µm into the Si.

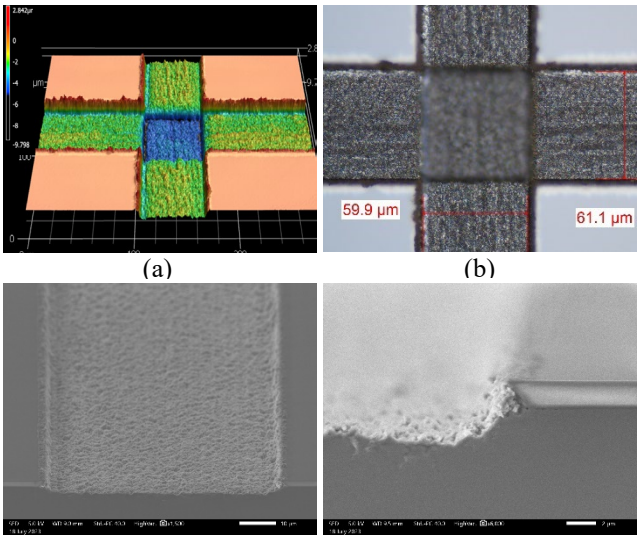

(a) (b) (c) (d)

Figure 7: Inspection of UV-USP laser grooved material shows a smooth groove bottom and a maximum of 300 nm burr with (a) confocal imaging and (b) optical microscopy. SEM inspection of a manually cleaved crosscut shows (c) a very flat groove bottom and zoomed in at the edge (d) reveals about 1.5 µm material modification at the top layer interface.

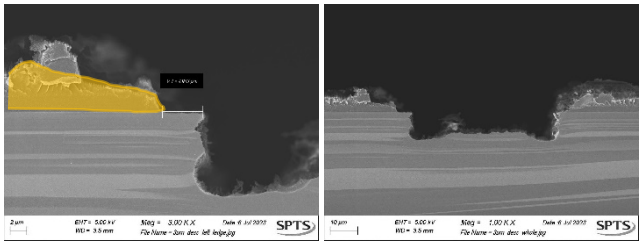

(a) (b)

Figure 8: The SEM image of (a) the UV-ns laser grooved material after descum (the coating is indicated in yellow) shows a pullback of the coating of up to 5 µm from the edge of the groove. In addition, a small modification at the interface of the top layer and silicon is visible. (b) SEM image of the overall groove profile.

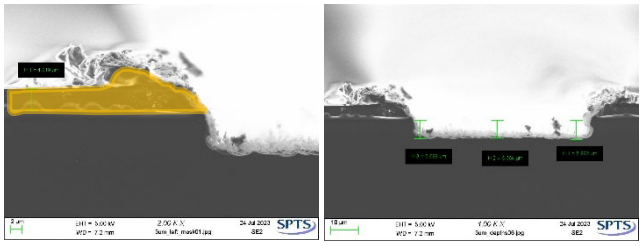

(a) (b)

Figure 9: The SEM image of (a) the UV-USP laser grooved material after descum (the coating is indicated in yellow) shows no coating pullback. The edge of the mask at the groove is sharp. (b) SEM image of the overall groove profile showing a light colored groove bottom which did not impact the plasma dicing process.

B. Plasma dicing of laser grooved Si with SiO_2 top

First, the plasma descum process step was varied to find the balance between sidewall quality without striations on the die sidewall and a minimum undercut and no lateral etch. After optimization, the descum deepens the groove with about 4 µm for both UV-ns and UV-USP laser processed samples, Fig. 8 and Fig. 9. For both samples, the bottom shape after descum is similar to the starting condition directly after laser grooving. However, a striking difference is the coating mask appearance: for UV-ns, the coating pullback is significant at both sides of the groove, measuring up to 5 µm. The UV-USP coating mask follows the groove edge more closely which is needed to protect the top layer during plasma dicing step. The UV-USP laser process produces less HAZ. This allows a more effective descum step, preventing the formation of striations and lateral etch during the plasma dicing step. The necessity of descum for these cases is shown in Fig. 10, where the plasma dicing without descum results in lateral etching, creating weak spots resulting in severe delamination of the top layer after the DI wash.

Plasma dicing of the UV-ns grooved sample shows 100% singulation. A soft landing was used for optimal backside quality. The sidewall of the sample has some irregularities and striations, Fig. 11a. The surface edge has no chipping or delamination, but the top surface has an irregularly sized modification at both sides of the groove of 10 to 16 µm. This

modification is hardly visible with optical microscope because of the layer transparency and the shallowness of the defect. It is expected that the surface change is the result of the coating mask pullback, exposing the surface to the plasma. SEM sidewall inspection shows about 1.1 µm burr at irregular locations at the die edge which can be a problem for hybrid bonding.

Figure 12 shows the result of plasma dicing the UV-USP laser grooved sample. The singulation was 100%. The samples showed a smooth sidewall without striations. The top surface has a regular modification at both sides of the die edge of up to 1.5 µm. A SEM inspection of the die sidewall showed up to 300 nm burr at irregular locations which is less than for UV-ns but can still be a problem for hybrid bonding.

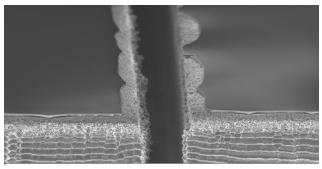

Figure 10: SEM images of plasma dicing after laser grooving without descum shows more than 10 µm delamination of the top layer.

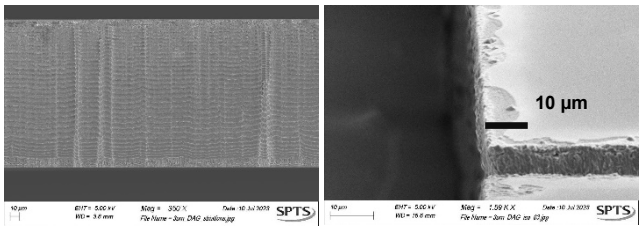

(a) (b)

Figure 11: SEM images of plasma dicing after UV-ns laser grooving showing (a) sidewall irregularities such as striations and (b) irregular top surface modification which is visible as the darker shaded areas along the die edge.

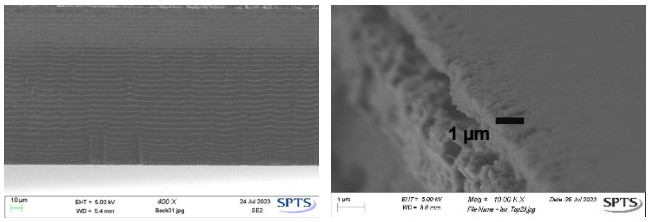

(a) (b)

Figure 12: SEM images of plasma dicing after UV-USP laser grooving showing (a) smooth sidewall without striations (b) a regular top surface with small modifications up to 1.5 µm.

C. *Die strength evaluation*

Fig. 13 shows a comparison of the die strength the UV-ns and UV-USP laser grooved and plasma diced samples. The material die strength was measured on a 3-point bending test tool with 15 samples per side. As can be seen from the graph, the UV-USP laser grooved samples show a slightly higher average for the front side than the UV-ns laser grooved samples. This indicates that the combination of UV-USP laser grooving and plasma dicing is a superior process.

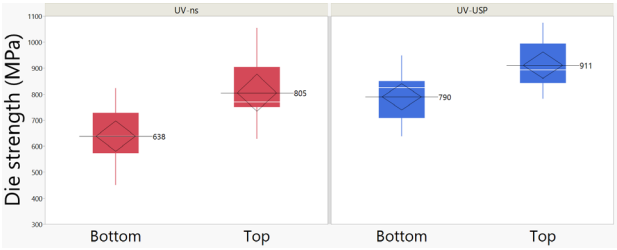

Figure 13: Die strength comparison of UV-ns and UV-USP laser grooved and plasma diced 150 µm Si with 2 um SiO_2.

Table 1: Comparison of the combination with plasma dicing of UV-ns laser grooving and UV-USP laser grooving.

Grooving laser	Burr (µm)	Modified surface (µm)	Die strength (MPa)	
			Top	Bottom
UV-ns	<1.1	>10	805	638
UV-USP	<0.3	<1.5	911	790

D. *Throughput consideration*

In the end, factors determining an effective production flow include considerations on overall capability, quality and throughput. Obviously, the combination of two technologies allows parallel processing for several of the process steps. As mentioned earlier, plasma dicing enables a narrow width, small die and high die strength singulation of non-rectangular shapes, with a particle free process. This does require a defined, sharp mask and the absence of metals in the separation lane. The laser as opposed to blade dicing can process a wide range of materials including metals consistently without the saw crack and delamination issues. The UV-USP laser approach, having a different material removal mechanism, has a reduced HAZ and lower burr, and shows a smooth groove bottom. Continuous optimization and improvement of UV-USP laser grooving combined with plasma dicing will contribute positively to attain both the highest quality with a high throughput at a low cost.

IV Conclusion

This study has shown the potential of the combination of UV-USP laser grooving versus UV-ns laser grooving, respectively combined with plasma dicing. UV-USP laser grooving shows a smoother groove profile and sidewall and a sharp, steep coating mask edge. This laser technology minimizes HAZ and descum shows better removal of recast and debris. After plasma dicing, the dies show no to minimal burr and in comparison, the die strength is higher for both front and backside of the die sample. The minimum

remaining surface burr of the UV-USP laser grooving process is completely removed by the subsequent plasma dicing step. The combination of UV-USP laser grooving and plasma dicing process is expected to meet the requirements for the hybrid bonding process flow. This study has shown that for the optimum quality of a singulated die for hybrid bonding, both processes have to be optimized with respect to each other. The quality benefits of the UV-USP laser system justify the higher cost of the UV-USP laser over the UV-ns laser.

As a next step, we will evaluate the complete removal of the burr followed by bonding tests. Afterwards, we will focus on further optimization using hybrid bonding product wafers including multiple layers in the dicing street with metal test structures.

Acknowledgment

We are grateful to M. van de Raa and P. Keukens for their contribution.

References

[1] W.-S. Lei, A. Kumar, and R. Yalamanchili, “Die singulation technologies for advanced packaging: A critical review,” *J. Vac. Sci. Technol. B,* vol. 30(4), Jul/Aug 2012, 040801.

[2] F. Inoue et al., “Advanced dicing technologies for the combination of wafer to wafer and collective die to wafer direct bonding,” *2019 IEEE 69tht Electronic Components and Technology Conference (ECTC),* 2019 pp. 437-445.

[3] R. Barnett, O. Ansell, and D. Thomas, “Considerations and benefits of plasma etch based wafer dicing, ” *2013 IEEE 15th Electronics, Packaging Technology Conference (EPTC)*, 2013, pp. 569–574.

[4] K. D. Mackenzie, D. Pays-Volard, L. Martinez, C.Johnson, T. Lazerand, and R. Westerman, ”Plasma-based Die Singulation Processing Technology ,” *2014 IEEE 64tht Electronic Components and Technology Conference (ECTC)*, 2014 pp. 1577-1583.

[5] F. Laermer, and A. Schilp, “Method of anisotropically etching silicon,” U.S. Patent 5 501 893, March 26, 1996

[6] M. Mark, “A review of laser ablation and dicing of Si wafers,” *Precision Eng.,* vol. 73, 2022, pp. 377–408.

[7] M. Domke et al., “Ultrafast-laser dicing of thin silicon wafers: strategies to improve front- and backside breaking strength,” *Applied Physics A*, vol. 123, no. 12, 2017, pp. 746-754.

[8] D. S. Finn, Z. Lin, J. Kleinert, M. J. Darwin, and H. Zhang, “Study of die break strength and heat-affected zone for laser processing of thin silicon wafers,” *Journal of Laser Applications*, vol. 27, no. 3, 2015, pp. 032004-1-7.

[9] Elsherbini et al., “Enabling next generation 3D heterogeneous integration architectures on Intel process,” *2022 IEEE International Electron Devices Meeting (IEDM)*, 2022, 2156-017X.

[10] J. van Borkulo, P. Verburg and R. Van Der Stam, "Multi beam full cut dicing of thin Si IC wafers," *2017 IEEE 67th Electronic Components and Technology Conference (ECTC)*, 2017, pp. 1817-182.

[11] S. Bertini et al., ”Scalloping and Stress Concentration in DRIE-Manufactured Comb-Drives,” *Actuators* Vol 7(3) 2018, pp. 57-79

[12] S. Schoenfelder, M. Ebert, C. Landesberger, K. Bock, and J. Bagdahn, “Investigations of the influence of dicing techniques on the strength properties of thin silicon,” *Microelectronics Reliability*, vol.47, no. 2–3, 2007, pp. 168–178.